

Evaluation of the safety factors of shotcrete linings during the creep stage

*Original*

Evaluation of the safety factors of shotcrete linings during the creep stage / Oreste, P., Spagnoli, G., Ramos, C.A.L.. - In: PROCEEDINGS OF THE INSTITUTION OF CIVIL ENGINEERS. GEOTECHNICAL ENGINEERING. - ISSN 1353-2618. - STAMPA. - 173:3(2020), pp. 274-282. [10.1680/jgeen.19.00104]

*Availability:*

This version is available at: 11583/2940954 since: 2021-11-28T17:29:10Z

*Publisher:*

ICE Publishing

*Published*

DOI:10.1680/jgeen.19.00104

*Terms of use:*

This article is made available under terms and conditions as specified in the corresponding bibliographic description in the repository

*Publisher copyright*

(Article begins on next page)

# Evaluation of the safety factors of shotcrete linings during the creep stage

Pierpaolo Oreste, PhD,<sup>1</sup> Giovanni Spagnoli, PhD, MBA<sup>2</sup>, Cesar Alejandro Luna Ramos, MSc<sup>3</sup>

<sup>1</sup> Full Professor, Department of Environmental, Land and Infrastructural Engineering, Politecnico di Torino, Corso Duca Degli Abruzzi 24, 10129 Torino, Italy, ORCID: 0000-0001-8227-9807

<sup>2</sup> Global Project and Technology Manager Underground Construction, BASF Construction Solutions GmbH, Dr.-Albert-Frank-Straße 32, 83308 Trostberg, Germany, *giovanni.spagnoli@basf.com*; (corresponding author), ORCID: 0000-0002-1866-4345

<sup>3</sup> Professor, Faculty of Engineering, Universidad Mariana, Faculty of Engineering, Universidad Mariana, Calle 18 No. 34-104, Pasto, Colombia, *celuna@umariana.edu.co*. Former MSc student at Department of Environmental, Land and Infrastructural Engineering, Politecnico di Torino, Corso Duca Degli Abruzzi 24, 10129 Torino, Italy

## Abstract

The sprayed concrete linings used in the tunnels generally develops secondary deformations over time even in the presence of constant stress levels within it. These deformations influence the loading process on the lining and, therefore, also the stress levels within the support structure. In this work the behaviour of the sprayed concrete linings in the tunnel was investigated, under different possible operating conditions, in order to evaluate the effect of secondary deformations over time on the evolution of stability conditions (safety margins with respect to the possible concrete failure) over time, after the construction of the tunnel has been completed. A parametric analysis has been performed to study 8 different types of tunnels, with variable geometry and rock quality, and 8 different types of sprayed concrete. 64 cases of the parametric analysis cover the vast range of variability of the influential parameters and allow to obtain useful considerations in relation to the effects of secondary deformations over time on the static behaviour of the lining and on the safety factor with reference to the possible failure of the sprayed concrete.

27 **KEY WORDS:** Tunnels & tunnelling; Excavation; Mathematical modelling

28

29 **Notation list**

- 30  $\varphi_p$ : peak friction angle of the rock;
- 31  $c_p$ : peak cohesion of the rock;
- 32  $c_r$ : residual cohesion of the rock;
- 33  $E_i$ : elastic modulus of shotcrete at  $i$ -th-step;
- 34  $E_{rm}$ : elastic modulus of the rock;
- 35  $E_\infty$ : elastic modulus of the shotcrete at infinity, when creep ceased;
- 36  $E_1$ : initial elastic modulus of the shotcrete at  $t = 0$ ;
- 37  $E_2$ : elastic modulus of the shotcrete in the parallel creep scheme;
- 38  $M$ : bending moments;
- 39  $N$ : normal forces;
- 40  $p_0$ : lithostatic pressure;
- 41  $R$ : tunnel radius;
- 42  $t_i$ : average time;
- 43  $t_{sc}$ : thickness of the shotcrete lining;
- 44  $\varphi_r$ : residual friction angle of the rock;
- 45  $\nu$ : Poisson coefficient of the rock;
- 46  $\nu_{sc}$ : Poisson coefficient of the shotcrete;
- 47  $\sigma_{ci}$ : uniaxial compressive strength;
- 48  $\sigma_{max,ci}$ : maximum compression stress in the lining, induced by the bending moments and by
- 49 the normal acting forces, in the  $i$ -th relief step;
- 50  $\sigma_{max,ti}$ : maximum tensile stress in the lining, induced by the bending moments and by the
- 51 normal acting forces, in the  $i$ -th relief step;
- 52  $\sigma_{ti}$ : tensile strength;
- 53  $\eta$ : viscosity of the shotcrete;
- 54  $\Psi$ : dilatancy of the rock;
- 55  $\alpha$ : rate of evolution of secondary deformations;

56  $\beta$  : ratio between the final secondary de-formations and the initial deformations;  
57  $k$  : ratio between the horizontal load and the vertical load applied to the lining;  
58  $k_i$ : average stiffness of the lining;  
59  $K_n$ : normal stiffness of the interaction spring between the lining and the rock (hyperstatic re-  
60 action method);  
61  $K_s$ : shear stiffness of the interaction spring between the lining and the rock (hyperstatic reac-  
62 tion method).  
63

64 **Introduction**

65 Sprayed concrete (or shotcrete) is concrete which is conveyed under high pressure through a  
66 pneumatic hose and projected into place at high velocity, with simultaneous compaction (DIN  
67 18551, 2005), see Fig. 1. Among the properties of shotcrete used for tunnel design, such as  
68 early (compressive) and long-time strength, tensile strength, shrinkage, curing time, cracking,  
69 durability, creep is one of the most important factors (Thomas, 2009), because shotcrete lin-  
70 ings are loaded at a very early age, therefore the influence of time dependent material proper-  
71 ties on the deformation behaviour and bearing capacity is much more significant than in regular  
72 concrete structures (Schädlich and Schweiger, 2014). Neville et al. (1983) define creep as the  
73 increase in strain with time under a sustained stress, i.e. the material deforms not only due to  
74 the stresses which it is subjected to, but also due over a time during which these stresses are  
75 applied.



76

77 **Fig. 1 Application of shotcrete**

78 According to Thomas (2009) the high creep capacity of sprayed concrete can be considered  
79 as positive as this can dissipate stress concentrations and avoid overloading. The current sim-  
80 plistic approach to model sprayed concrete linings in numerical simulations assumes a linear  
81 elastic material with a stepwise increase of the Young's modulus in subsequent excavation  
82 stages in order to simulate the curing effect. While realistic lining deformations may be obtained  
83 with this method, lining stresses are usually too high, in particular if the lining is subjected to  
84 significant bending (Schädlich and Schweiger 2014). For sprayed concrete, the principle of  
85 rheological models are the same as for rock (Thomas 2009). However, in shotcrete creep is  
86 significantly higher at an early stage of load as the strength of concrete is lower, as found by  
87 Huber (1991). However, it must be kept in mind that some accelerators increase the early  
88 strengths (Melbye 1994) therefore creep after 24 or 48 h is close to that at greater ages (Ku-  
89 wajima, 1999). Concrete reinforcement reduces creep, presumably due to the restrain effect  
90 (Ding, 1998). However, reinforcing synthetic fibers sprayed together with the shotcrete have  
91 twice the creep capacity than a shotcrete with steel fibres (Thomas, 2009; MacKay and Trottier,  
92 2004).

93 Numerical models are massively employed to analyse the creep behaviour of shotcrete linings  
94 such as some rheological models (Jaeger and Cook, 1979): Kelvin model (Neville et al., 1983;  
95 Jaeger and Cook, 1979; Rokahr and Lux, 1987), Burgers model (Yin, 1996), viscoplastic model  
96 (Thomas, 2009). Kelvin creep model produces a complete recovery, unlike the Maxwell models  
97 where no recovery is produced. The rheological models help to give a better understanding of  
98 the visco-elastics and elasto-viscoplastics behavior. However, these models do not account  
99 for shear stresses, temperature and intrinsic structure. Regarding the power laws creep model  
100 for sprayed concrete, of the three stages of creep, only primary creep is of interest for sprayed  
101 concrete linings after construction (Thomas 2009). Several authors used the power laws for  
102 sprayed concrete lining tunnels (e.g. Schubert, 1988; Yin, 1996), however according to  
103 Thomas (2009) they are not widely used because of their inferior ability to model complex  
104 creep behaviour. It has to be pointed out, that real creep behaviour of linings is hard to obtain  
105 as the load-bearing system is a composite consisting of the ground and the lining. Therefore,

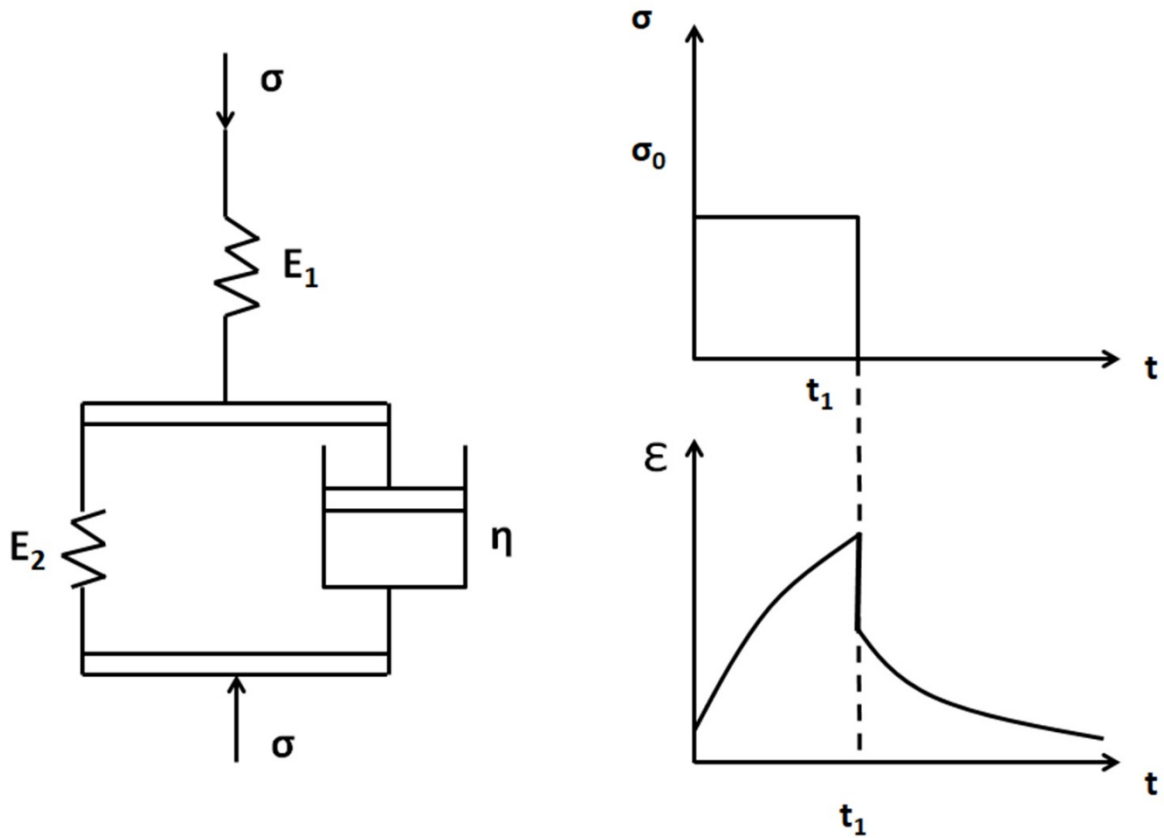
106 the reduction in the lining stress due to the creep depends on the characteristics of the sur-  
107 rounding ground (Thomas 2009). As observed by Pöttler (1990) and Yin (1996) if the ground  
108 is modelled as elastoplastic, the load on the lining can increase following creep.

109 This research shows a parametric analysis considering a novel model based on the hyperstatic  
110 reaction model (HRM) and the convergence-confinement method (CCM), based on the Voigt-  
111 Kelvin creep model (Oreste et al. 2019), considering eight types of tunnels, 8 types of concrete  
112 and two rock types. CCM (Oreste, 2009; 2015; Spagnoli et al., 2016; 2017) is able to evaluate  
113 the initial load on the sprayed concrete lining, through the intersection of the convergence-  
114 confinement curve (CCC) with the reaction line of the lining, considering initial elastic modulus  
115 of the shotcrete ( $E_1$ ) before the creep takes place. HRM investigates the behaviour of SC lining  
116 under the loads applied by the surrounding rock and considering the correct interaction be-  
117 tween the lining and the rock (Oreste, 2007, Do et al., 2014a; 2014b). The HRM considers half  
118 of a tunnel section by beam elements connected by nodes. The elements develop bending  
119 moments, axial forces and shear forces. The interaction between ground and support is rep-  
120 resented by “Winkler” type springs in the normal and tangential direction for each node of the  
121 model (Oreste et al., 2018; 2019b).

## 122 **The numerical model used to study the creep behaviour of a shotcrete lining**

123 The numerical model adopted (Oreste et al., 2019a) permits to consider the secondary defor-  
124 mation behaviour of a sprayed concrete lining in the time following the construction of the  
125 tunnel, evaluating in detail the stress transmitted from the rock to the tunnel boundary. The  
126 simplification scheme of Voigt-Kelvin was used in the calculation (Figure 2):

$$127 \quad \varepsilon_t = \frac{\sigma}{E_2} \cdot \left(1 - e^{-\frac{E_2 \cdot t}{\eta}}\right) + \frac{\sigma}{E_1} \quad (1)$$



128

129 **Fig. 2 Voigt-Kelvin creep model ( $\sigma$  is the applied load,  $E$  is the elastic modulus and  $\eta$  is**  
 130 **the viscosity coefficient,  $\varepsilon$  is the deformation.**

131 This scheme allows to analyse the evolution of secondary deformations over time (rate de-  
 132 pending on the term  $E_2$  and viscosity  $\eta$ ) through a progressive reduction of the elastic modulus  
 133 representative of the sprayed concrete, starting from an initial value  $E_1$  (at the end of the phase  
 134 tunnel construction) up to a lower value  $E_\infty$  which characterizes the support structure at time  
 135  $t=t_\infty$  after the tunnel construction phase has ended. The following relation applies (Oreste et  
 136 al., 2019):

$$137 \quad \frac{1}{E_\infty} = \frac{1}{E_1} + \frac{1}{E_2} \quad (2)$$

138 Defining the final secondary deformations, due to the creep, as a certain percentage  $\beta$  of the  
 139 primary deformations (the initial ones), we have:  $E_2 = E_1/\beta$ , and, therefore:  $E_\infty = \frac{E_1}{(1+\beta)}$ .

140 Knowing the values  $E_1$  and  $E_\infty$ , it is possible to determine the initial ( $k_{in}$ ) and final ( $k_{fin}$ ) stiff-  
 141 ness of the lining and evaluate, through the Convergence-Confinement Method (CCM), the  
 142 reduction of the load applied by the rock to the support structure during the evolution of the  
 143 secondary deformations in the shotcrete (Oreste et al., 2019). The phenomenon of reduction  
 144 of the applied load is simulated for homogeneous steps and to each of them is associated a  
 145 value of the average stiffness of the lining,  $k_i$ , a value of the average elastic modulus  $E_i$  of the  
 146 sprayed concrete (equation 3), and finally a value of the average time,  $t_i$ , following the com-  
 147 pletion of the tunnel construction in the studied section (equation 4):

$$148 \quad E_i = \frac{k_i \cdot (1 + v_{sc}) \cdot [(1 - 2 \cdot v_{sc}) \cdot R^2 + (R - t_{sc})^2] \cdot R}{R^2 - (R - t_{sc})^2} \quad (3)$$

$$149 \quad t_i = \frac{-\eta \cdot \ln\left[\left(\frac{E_2}{E_1}\right) + 1 - \left(\frac{E_2}{E_i}\right)\right]}{E_2} \quad (4)$$

150 Once these parameters have been determined for each unloading step, it is possible to use  
 151 the Hyperstatic Reaction Method (HRM) to verify the stress in the sprayed concrete produced  
 152 by secondary deformations over time. More specifically, we start from considering the devel-  
 153 opment of bending moments, normal forces and shear forces in the initial situation (at the end  
 154 of the tunnel construction phase) and the stress state is modified in relation to the effects pro-  
 155 duced by the applied relief load steps. Each relief step is applied to a lining that appears with  
 156 a different elastic module,  $E_i$ , gradually decreasing. At the end of the calculation the final load  
 157 state is obtained, associated with a very large time,  $t_i$ , representative of the final phase of the  
 158 secondary deformation process.

159 Since shotcrete shows an overall reduction of the elastic modulus ( $E_i$ ) over time ( $t_i$ ) due to the  
 160 development of secondary deformations (creep), it is possible to associate to the value  $E_i$  also  
 161 the unconfined compressive strength of the sprayed projected ( $\sigma_{ci}$ ) and the tensile strength  
 162 ( $\sigma_{ti}$ ). In general, the strength values follow the same pattern over time as shown by the elastic  
 163 modulus and it is therefore possible to assume the constant ratio ( $E_i/\sigma_{ci}$  and  $E_i/\sigma_{ti}$ ) over time  
 164 between the modulus of elasticity and the strength of the shotcrete. This assumption allows to  
 165 determine over time the safety factor of the lining ( $FS$ ), considered as the ratio between the

166 maximum acting stress (induced in the shotcrete by the bending moment and the normal force)  
167 and the strength of the sprayed concrete. There are two safety factors, one related to the  
168 possible cracking of the shotcrete by compression ( $FS_{,ci}$ ), the other related to the possible  
169 tensile failure ( $FS_{,ti}$ ), only if the combination of bending moments and normal forces induces  
170 (at least in a portion of the lining) tensile stresses:

$$171 \quad FS_{,ci} = \sigma_{ci} / \sigma_{max,ci} \quad (5)$$

$$172 \quad FS_{,ti} = \sigma_{ti} / \sigma_{max,ti} \quad (6)$$

173 Where:

174  $\sigma_{max,ci}$  is the maximum compression stress in the lining, induced by the bending moments and  
175 by the normal acting forces, in the i-th relief step;

176  $\sigma_{max,ti}$  is the maximum tensile stress in the lining (if it exists), induced by the bending moments  
177 and by the normal acting forces, in the i-th relief step.

178 Being able to obtain the trend of the safety factors of the shotcrete for each relief step, it is  
179 possible to evaluate the stability conditions of the lining over time, during the evolution of the  
180 secondary deformation process. This circumstance is very useful for checking the effects of  
181 the creep on the stability conditions of the shotcrete tunnel linings.

## 182 **The parametric analysis on the effect of creep on the behaviour of a shotcrete lining**

183 In order to theoretically analyse the effect of the creep on the mechanical behaviour of a  
184 sprayed concrete lining, a parametric study was developed in which 8 different types of circular  
185 tunnel were considered, which differ in geometry (diameter), geomechanical quality (RMR) of  
186 the rock in which they are excavated and lithostatic stress state ( $p_0$ ), which depends on the  
187 depth of the tunnel. The 8 types of tunnel are obtained by combining this set of pairs of values:

- 188 • Tunnel radius,  $R$ : 2m and 6m;
- 189 • RMR index of the rock: 30 and 60
- 190 • Lithostatic stress state,  $p_0$ : 2MPa and 7MPa.

191 RMR of 30 and 60 were considered in order to have a wide range of mechanical parameters  
 192 of the rock, typical of situations where SC linings are used. Table 1 shows the values of the  
 193 geomechanical parameters of the rock arbitrary assumed for each of the two values of the  
 194 RMR quality index. The initial stiffness of the normal and shear springs ( $K_n$  and  $K_n$  respec-  
 195 tively) are usually evaluated from the rock data using very simple relationships (Oreste, 2007):

$$K_n = \frac{2 \cdot E_{rm}}{R} \quad (7)$$

$$K_n = 0.5 \cdot K_n \quad (8)$$

196 Where  $E_{rm}$  is the elastic modulus of the rock and  $R$  is the tunnel radius.

197 **Table 1 Geomechanical parameters of the rock assumed in the calculation for the two**  
 198 **values of the RMR indices considered in the parametric analysis.**

| <b>RMR 30</b>                        |                         |              |
|--------------------------------------|-------------------------|--------------|
| <b>Rock parameter</b>                | <b>Unity of measure</b> | <b>Value</b> |
| Elastic modulus ( $E_{rm}$ )         | [MPa]                   | 3160         |
| Coefficient of Poisson ( $\nu$ )     | [-]                     | 0.30         |
| Peak cohesion ( $c_p$ )              | [MPa]                   | 0.15         |
| Residual cohesion ( $c_r$ )          | [MPa]                   | 0.12         |
| Peak friction angle ( $\phi_p$ )     | [°]                     | 20           |
| Residual friction angle ( $\phi_r$ ) | [°]                     | 16           |
| Dilatancy ( $\psi$ )                 | [°]                     | 16           |
| $K_n$                                | [MN/m]                  | 550.82       |

|   |                         |              |
|---|-------------------------|--------------|
| $K_s$                                   | [MN/m]                  | 275.41       |
| <b>RMR 60</b>                           |                         |              |
| <b>Rock parameter</b>                   | <b>Unity of measure</b> | <b>Value</b> |
| Elastic modulus ( $E_{rm}$ )            | [MPa]                   | 17780        |
| Coefficient of Poisson ( $\nu$ )        | [-]                     | 0.30         |
| Peak cohesion ( $c_p$ )                 | [MPa]                   | 2            |
| Residual cohesion ( $c_r$ )             | [MPa]                   | 2            |
| Peak friction angle ( $\varphi_p$ )     | [°]                     | 37           |
| Residual friction angle ( $\varphi_r$ ) | [°]                     | 37           |
| Dilatancy ( $\psi$ )                    | [°]                     | 16           |
| $K_n$                                   | [MN/m]                  | 3099.26      |
| $K_s$                                   | [MN/m]                  | 1549.63      |

199

200 8 different types of sprayed concrete were then considered, in relation to the possibility of  
201 developing secondary deformations over time. The types of shotcrete differ in terms of the  
202 value of the initial elastic modulus ( $E_1$ ), the parameter  $\beta$  (ratio between the final secondary de-  
203 formations and the initial deformations) and the rate with which secondary deformations evolve  
204 over time (secondary deformations after 3 years equal to half or one third of the final secondary  
205 deformations):

- 206 • Initial elastic modulus  $E_1$  of the sprayed concrete: 8000 MPa and 16000 MPa

- 207 • Parameter  $\beta$  (ratio between the final secondary deformations and the initial defor-
- 208 mations): 0.33 and 1.
- 209 • Rate of evolution of secondary deformations: secondary deformations after 3 years
- 210 from the construction ending of the tunnel equal to  $\alpha=1/3$  or  $\alpha =1/2$  times the final sec-
- 211 ondary deformations (for a very long time).

212 The combination of three pairs of values leads to 8 different types of concrete. Each of these

213 ones was considered in each of the 8 tunnel types mentioned above. In total, therefore, 64

214 different cases were analysed.

215 Table 2 and 3 summarize the characteristic values of the 8 types of tunnel considered and the

216 8 types of shotcrete hypothesized in the calculation, respectively. The viscosity  $\eta$  is calculated

217 using equation 1 which describes the path of the deformations over time:

218 
$$\eta = -\frac{E_2 \cdot (3 \cdot 3600 \cdot 24 \cdot 365)}{\ln(1-\alpha)} \quad (9)$$

219 **Table 2 Types of tunnel considered in the developed parametric analysis.**

| Sequence | RMR | Tunnel radius, $R$ (m) | Lithostatic stress state, $p_0$ (MPa) |
|----------|-----|------------------------|---------------------------------------|
| A        | 30  | 2                      | 2                                     |
| B        | 30  | 2                      | 7                                     |
| C        | 30  | 6                      | 2                                     |
| D        | 30  | 6                      | 7                                     |
| E        | 60  | 2                      | 2                                     |
| F        | 60  | 2                      | 7                                     |
| G        | 60  | 6                      | 2                                     |

|   |    |   |   |
|---|----|---|---|
| H | 60 | 6 | 7 |
|---|----|---|---|

220

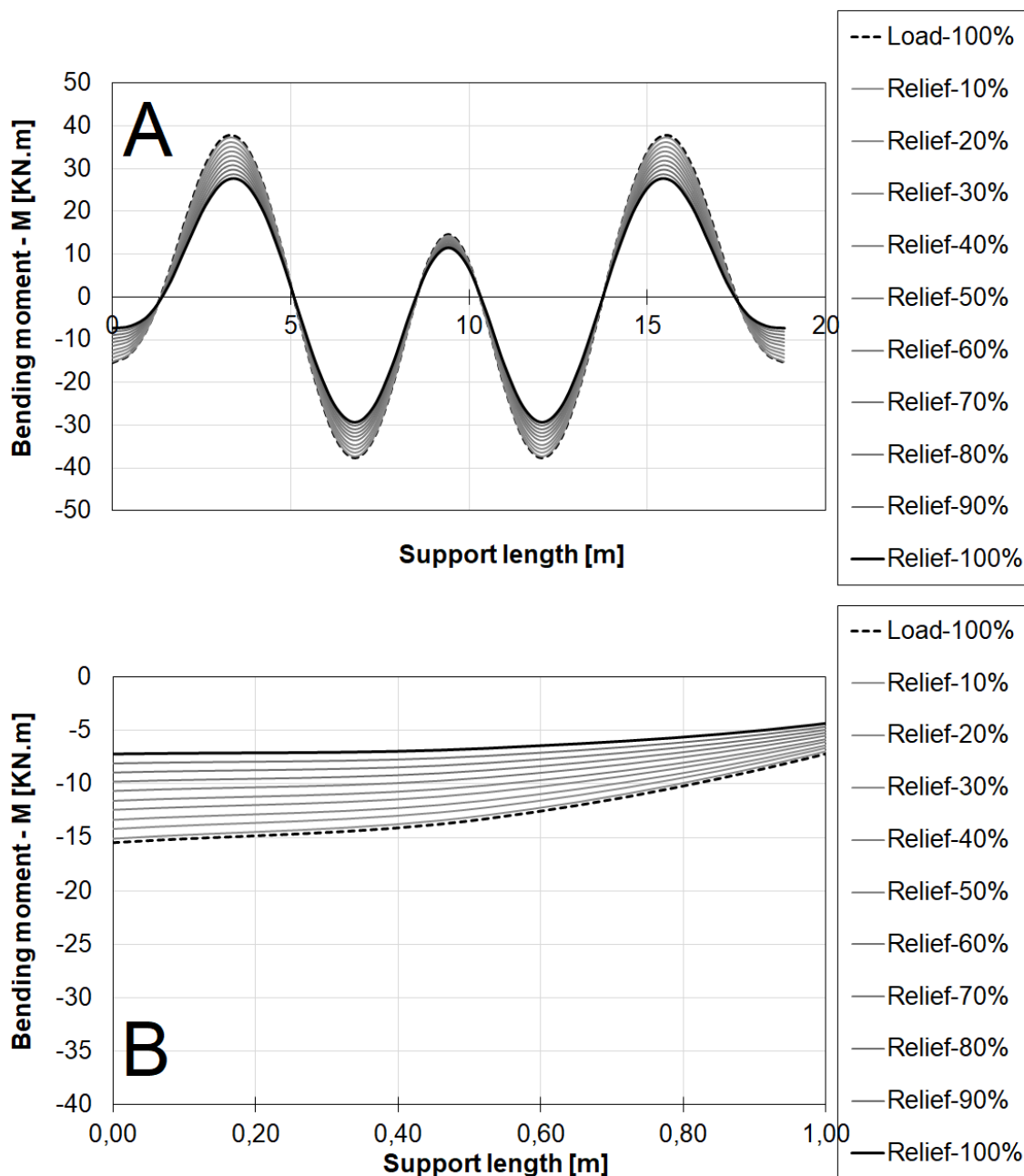
221 **Table 3 Types of sprayed concrete considered in the developed parametric analysis.**

| Case | Initial elastic modulus of the shotcrete at $t = 0, E_1$ (MPa) | Elastic modulus of the shotcrete in the parallel creep scheme, $E_2$ (MPa) | Viscosity $\eta$ (MPa·s) | $\alpha$ parameter | $\beta$ parameter |
|------|--|--|--------------------------|--------------------|-------------------|
| 1    | 8000   | 24000  | $2.067 \times 10^{12}$   | 0.5                | 0.33              |
| 2    | 8000   | 24000  | $3.276 \times 10^{12}$   | 0.33               | 0.33              |
| 3    | 8000   | 8000   | $6.889 \times 10^{11}$   | 0.5                | 1                 |
| 4    | 8000   | 8000   | $1.092 \times 10^{12}$   | 0.33               | 1                 |
| 5    | 16000  | 48000  | $4.134 \times 10^{12}$   | 0.5                | 0.33              |
| 6    | 16000  | 48000  | $6.552 \times 10^{12}$   | 0.33               | 0.33              |
| 7    | 16000  | 16000  | $1.378 \times 10^{12}$   | 0.5                | 1                 |
| 8    | 16000  | 16000  | $2.184 \times 10^{12}$   | 0.33               | 1                 |

222

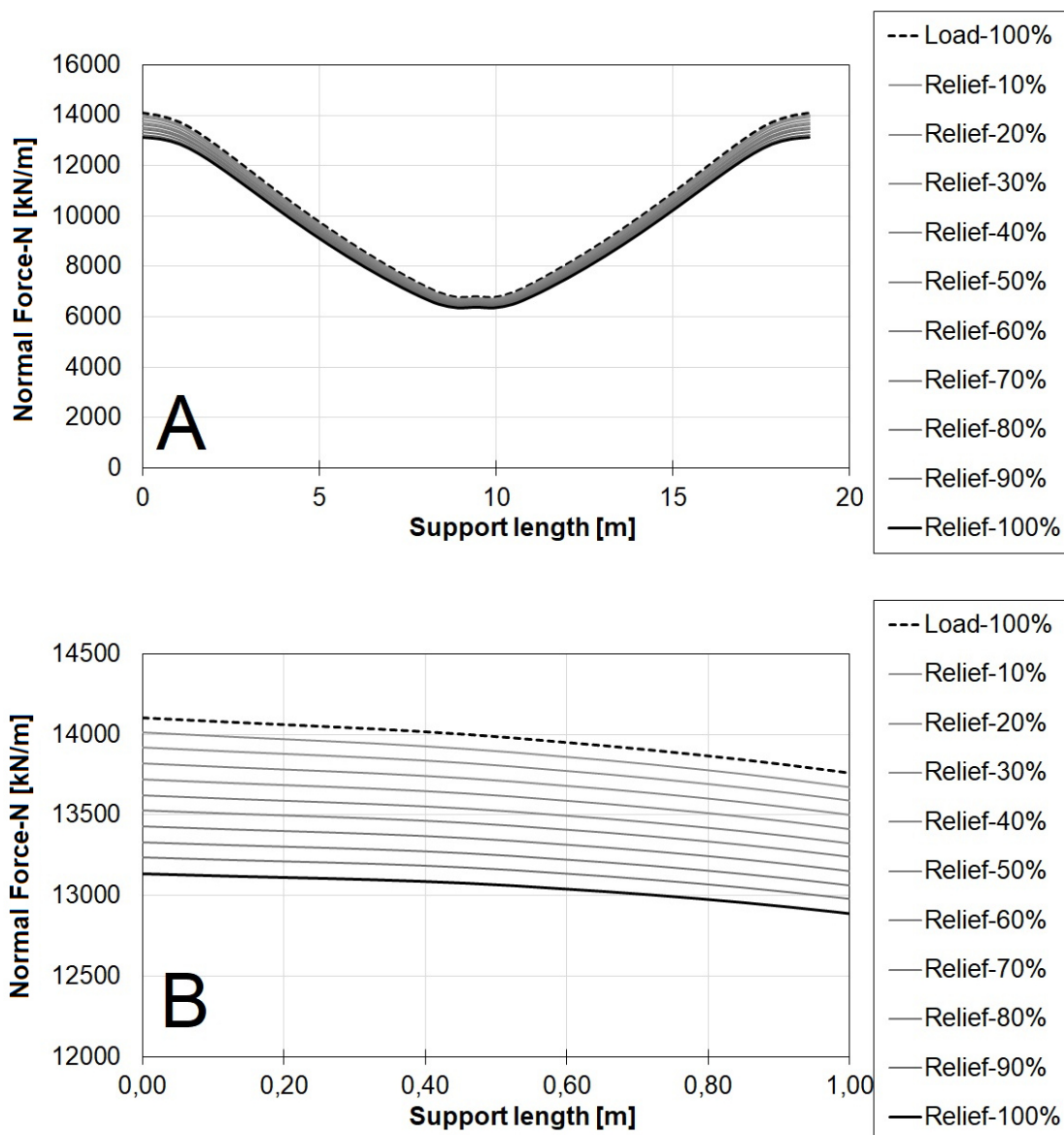
223 The thickness of the sprayed concrete lining,  $t_{sc}$ , was set at 0.2 m and the Poisson ratio,  $\nu_{sc}$ ,  
 224 was 0.15. The ratio  $k$  between the horizontal load and the vertical load applied to the lining  
 225 was considered equal to 0.5. The time associated with the decrease of the elastic modulus  
 226 corresponding to the midpoint of each of the 10 steps is thus obtained. With the proposed  
 227 model it is possible to conduct studies in terms of variations of normal and shear forces, rota-  
 228 tion and bending moments. For each of the 64 cases studied it was possible to obtain the trend  
 229 of the bending moments  $M$  and of the normal forces  $N$  along the development of the lining in

230 a transverse section of the tunnel. Figures 3 and 4 show, as an example, respectively the  
 231 values of the trend of the bending moment and of the normal force along the support structure  
 232 (for half of its development in the cross section, starting from the centre of the reverse arc of  
 233 the tunnel) for the case D1 (type D tunnel, type 1 shotcrete-see Tab. 2 and 3).



234  
 235 **Fig. 3 Trend of bending moments along the development of the shotcrete lining, in a**  
 236 **tunnel cross section, for the D1 case studied in the parametric analysis (A). Detail for**  
 237 **the first meter of support length (B). The origin of the lines refers to the centre of the**

238 reverse arc and the diagrams consider half of the development of the supporting struc-  
 239 ture. The diagram shows the trend at the end of the tunnel construction phase ( $t = 0$ ),  
 240 with the dotted line, and for the 10 stress relief steps considered, until reaching a very  
 241 high time value (for which  $E_i \approx E_\infty$ ,  $t \approx \infty$ ), shown with the continuous black line.



242  
 243 **Fig. 4** Trend of normal forces along the development of the shotcrete lining, in a tunnel  
 244 cross section, for the D1 case studied in the parametric analysis (A). Detail for the first  
 245 meter of support length (B). The origin of the lines refers to the centre of the reverse arc  
 246 and the diagrams consider half of the development of the supporting structure. The  
 247 diagram shows the trend at the end of the tunnel construction phase ( $t = 0$ ), with the

248 **dotted line, and for the 10 stress relief steps considered, until reaching a very high time**  
249 **value (for which  $E_t \approx E_\infty$ ,  $t \approx \infty$ ), shown with the continuous black line.**

250 From the analysis of the results shown in Figs. 3 and 4 it can be seen how the creep phenom-  
251 enon can lead, depending on the type of tunnel (diameter, depth and quality of the rock) and  
252 the type of sprayed concrete (initial stiffness, entity final of secondary deformations and vis-  
253 cosity), to significant changes in the trend of bending moments and normal forces induced  
254 along the development of the lining. The variation of the maximum bending moment along the  
255 lining and of the normal force at the point of maximum moment is interesting. Starting from the  
256 values of  $M$  and  $N$ , the stress induced in the sprayed concrete at each point of the lining and,  
257 therefore, the maximum value of stress, among those present was determined. In the following,  
258 reference will be made only to the analysis with respect to the compression stress, since no  
259 tensile stresses were detected within the lining in any of the examined cases. Because the  
260 failure of the sprayed concrete linings can occur in compression or traction, it is useful to eval-  
261 uate the maximum compressive stresses and the maximum tensile stresses reached at each  
262 stage during the creep phase and compare them with the compressive and tensile strength.  
263 While the compression stress is always present in a tunnel support, it is not always possible  
264 to detect the traction stress, or the traction stress does not always reach levels such as to be  
265 close to the tensile strength of the shotcrete. The evaluation of the maximum compression  
266 tension  $\sigma_{max,ci}$  (equation 5) in the shotcrete lining referred to the combined compressive and  
267 bending stress:

$$268 \sigma_{max,ci} = \max \left( 6 \cdot \frac{|M|}{1 \cdot t^2} + \frac{|N|}{1 \cdot t} \right) \quad (10)$$

269 where  $M$  and  $N$  are the values of bending moment and normal force which are present at the  
270 same point along the circumferential development of the supporting structure.

271 Starting from  $\sigma_{max,ci}$ , it was then possible to determine the safety factor  $FS$ , (equation 5), in  
272 order to evaluate the compressive strength  $\sigma_{ci}$  variable over time and linked to the value of the  
273 elastic modulus  $E_i$  determined at each single relief step considered. For the determination of  
274  $\sigma_{ci}$  reference was made to the Chang and Stille equation (1993):

275 
$$\sigma_{ci} = \left( \frac{E_i}{3.86} \right)^{\frac{5}{3}} \quad (11)$$

276 where  $E_i$  is the elastic modulus in GPa and  $\sigma_{ci}$  is uniaxial compressive strength of the shotcrete  
277 in MPa.

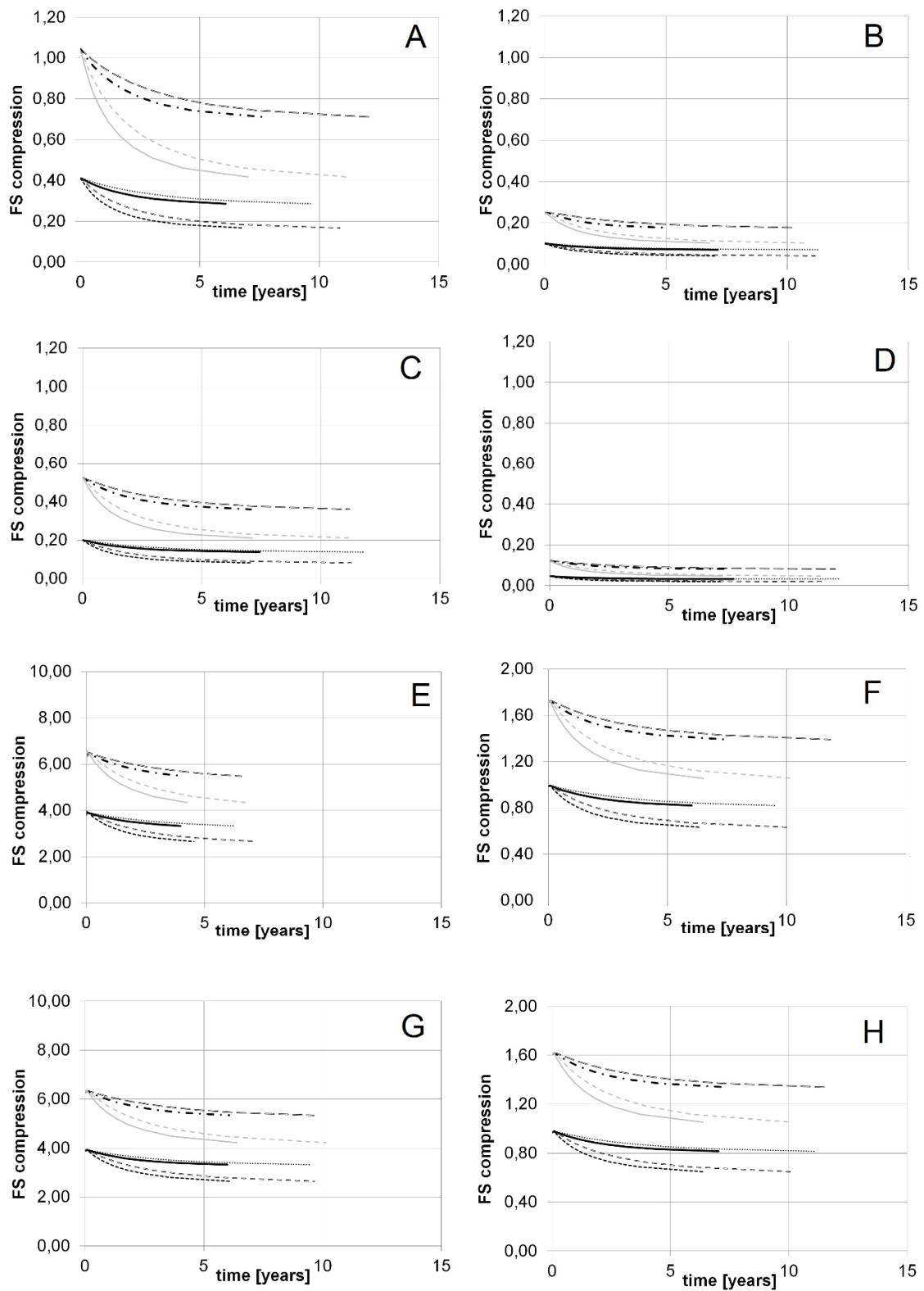
278 In the specific case, 10 stress relief steps were considered and, therefore, for each of them the  
279 load reduction value (vertical and horizontal) applied to the lining, the elastic modulus  $E_i$   
280 reached by the shotcrete in that specific step and, consequently, the strength  $\sigma_{ci}$  of the shot-  
281 crete were determined.

282 For each of the 64 cases studied the safety factor of the lining at the time variation  $t_i$  was  
283 determined. In all cases a reduction in the safety factor over time was found, starting from the  
284 value found at the end of the tunnel construction phase, when the time  $t$  was conventionally  
285 set to 0. The minimum value of the factor safety is always reached at the end of the creep  
286 phase, for very long times,  $t$ . During the design of the lining, it is possible to keep the attention  
287 on the value of the safety factor for a time  $t = t_{\infty}$ , when its minimum value is reached.

288 Fig. 5 (A-H) shows the results obtained for the safety factor of the lining during the creep phase  
289 for the 8 considered tunnels (A-H, see Tab. 2).

290 The trends referring to the 8 types of shotcrete considered are illustrated for each tunnel. The  
291 analysis of the graphs shows how the initial safety factor (at the end of the tunnel construction  
292 phase) depends for each tunnel on the elastic form  $E_1$  of the sprayed concrete only. The other  
293 parameters characterizing the shotcrete ( $E_2$  and  $\eta$ ) have no role. The percentage reduction of  
294 the final safety factor (at the end of the creep phase), with respect to the initial value, on the  
295 other hand, depends on the elastic modulus  $E_2$ , i.e. on the elastic modulus indicating the overall  
296 entity of the secondary deformations. The reduction of the safety factor due to the phenomenon  
297 of creep can be very consistent, especially for low values of the geomechanical quality index  
298 of the rock and for shallow tunnels.

299 The viscosity only influences the rate with which the final condition with minimum safety factor  
300 is reached in time: obviously, with increasing viscosity, the time necessary to reach the mini-  
301 mum safety factor increases.



|         |         |         |         |
|---------|---------|---------|---------|
| -Case 1 | -Case 2 | -Case 3 | -Case 4 |
| -Case 5 | -Case 6 | -Case 7 | -Case 8 |

304 **Fig. 5 Trend of safety factors over time at the tunnels type A to H, for the 8 types of**  
305 **sprayed concrete considered.**

306 From the analysis of the results of the parametric analysis it is possible to note, therefore, how  
307 the creep phenomenon can be very important for the behaviour of the sprayed concrete lining  
308 of a tunnel and, therefore, cannot be neglected in the design phase. The determination of the  
309 minimum safety factor, at the end of the creep phase is interesting. In fact, this value influences  
310 the design of the supporting structure and must be determined during calculation. In order to  
311 correctly evaluate the minimum safety factor, it is necessary to estimate the elastic modulus  
312  $E_2$  of the shotcrete in the simplified Voigt-Kelvin model. This parameter is determined starting  
313 from the estimate of the final entity of the secondary deformations of the sprayed concrete with  
314 respect to the initial deformations obtained at the end of the tunnel construction phase. In order  
315 to have an estimate of  $E_2$ , it is therefore useful to evaluate the evolution of secondary defor-  
316 mations for a certain period of time for a specimen of shotcrete in laboratory.

### 317 **Conclusions**

318 In this work, after having framed the problem of creep in shotcrete, the result of a parametric  
319 study obtained using a specific calculation tool, developed to study this particular mechanical  
320 phenomenon, is presented. This calculation tool uses the convergence-confinement method  
321 and the hyperstatic reaction method and allows to evaluate the evolution of the stresses and  
322 deformations of the sprayed concrete lining over time, in order to determine its safety factor  
323 conditions with respect to stability. A simplified model of creep, i.e. the Voigt-Kelvin model, was  
324 considered to represent the behaviour of the sprayed concrete. The parametric analysis has  
325 considered different types of tunnels, different in diameter, depth and type of rock, and different  
326 types of shotcrete. In all the cases analysed a reduction in the safety factor over time was  
327 noted, showing the importance of the creep study for the correct design of the thickness of the  
328 sprayed concrete lining. The final value of the safety factor is therefore fundamental for the  
329 design phase of the tunnel support. This value depends in particular on the elastic modules  
330 which the sprayed concrete has in the initial phase and during the evolution of the secondary

331 deformations. The percentage reduction of the final safety factor (at the end of the creep  
332 phase), with respect to the initial value, depends on the elastic modulus indicating the overall  
333 entity of the secondary deformations. The reduction of the safety factor due to the phenomenon  
334 of creep can be very consistent, especially for low values of the geomechanical quality index  
335 of the rock and for shallow tunnels. The viscosity is useful only to predict the time necessary  
336 to reach the final condition in which the secondary deformations can be considered accom-  
337 plished. For the correct design of the sprayed concrete lining it is essential to define some  
338 parameters influencing the creep behaviour of the material: in particular, in addition to the initial  
339 elastic modulus, which influences the initial deformations of the lining, it is necessary to eval-  
340 uate the final entity secondary deformations and in particular the ratio between the final sec-  
341 ondary deformations and the initial deformations obtained at the end of the tunnel construction  
342 phase.

#### 343 **References**

344 Chang Y, Stille H (1993) Influence of early age properties of shotcrete on tunnel construction  
345 sequences. In Wood, D.F., Morgan, D.R. (Eds.), Shotcrete for Underground Support VI, Amer-  
346 ican Society of Civil Engineers, Reston, pp. 110-117.

347 DIN 18551-01 (2005) Spritzbeton - Anforderungen, Herstellung, Bemessung und Konformität.  
348 Beuth Verlag GmbH, Berlin.

349 Ding Y (1998) Technologische Eigenschaften von jungen Stahlfaserbeton und Stahlfaser-  
350 spritzbeton. PhD thesis, University of Innsbruck (Austria).

351 Do, N.A., Dias, D., Oreste, P., and Djeran-Maigre, I (2014a) The behavior of the segmental  
352 tunnel lining studied by the hyperstatic reaction method. *European Journal of Environmental  
353 and Civil Engineering* 18(4), 489–510.

354 Do, N.A., Dias, D., Oreste, P., and Djeran-Maigre, I (2014b) The Influence of the Simplified  
355 Excavation Method on Tunnel Behaviour. *Geotechnical and Geological Engineering* 32(1), 43-  
356 58.

357 Hellmich C, Mang HA (1999) Influence of the dilation of soil and shotcrete on the load bearing  
358 behaviour of NATM-Tunnels. *Felsbau* 17:35-43.

359 Huber HG (1991) Untersuchung zum Verformungsverhalten von jungem Spritzbeton im Tun-  
360 nelbau. Master thesis, University of Innsbruck (Austria).

361 Jaeger JC, Cook NGW (1979) *Fundamentals of Rock Mechanics*. London: Chapman and Hall.

362 Kuwajima FM (1999) Early age properties of the shotcrete. In Celestino T, Parker, H, eds.  
363 *Shotcrete for Underground*, Sao Paulo, Brazil, 153–173.

364 MacKay J, Trottier JF (2004) Post-crack creep behaviour of steel and synthetic FRC under  
365 flexural loading. In Bernard ES, ed. *Shotcrete: More Engineering Developments*. London: Tay-  
366 lor & Francis, 183-192.

367 Melbye T (1994) *Sprayed Concrete for Rock Support*. Switzerland: MBT Underground Con-  
368 struction Group.

369 Neville AM, Dilger WH, Brooks JJ (1983) *Creep of plain and structural concrete*, Harlow: Con-  
370 struction Press.

371 Oreste P (2007) A numerical approach to the hyperstatic reaction method for the dimensioning  
372 of tunnel supports. *Tunnelling and Underground Space Technology* 22(2):185–205,  
373 <https://doi.org/10.1016/j.tust.2006.05.002>.

374 Oreste P (2009) The Convergence-Confinement Method: Roles and limits in modern geome-  
375 chanical tunnel design. *American Journal of Applied Sciences* 6(4):757-771.

376 Oreste P (2015) Analysis of the Interaction between the Lining of a TBM Tunnel and the  
377 Ground Using the Convergence-Confinement Method. *American Journal of Applied Sciences*  
378 12(4):276-283. DOI: 10.3844/ajassp.2015.276.283.

379 Oreste P, Spagnoli G, Luna Ramos CA, Seville L (2018) The Hyperstatic Reaction Method for  
380 the Analysis of the Sprayed Concrete Linings Behavior in Tunneling. *Geotechnical and Geo-*  
381 *logical Engineering*, 36(4): 2143–2169, <https://doi.org/10.1007/s10706-018-0454-6>.

382 Oreste P, Spagnoli G, Ceravolo LA (2019a) A numerical model to assess the creep of shotcrete  
383 linings. *Proceedings of the Institution of Civil Engineers – Geotechnical Engineering*, 172(4),  
384 344-354, <https://doi.org/10.1680/jgeen.18.00089>.

385 Oreste P, Spagnoli G, Luna Ramos CA (2019b) The Elastic Modulus Variation During the  
386 Shotcrete Curing Jointly Investigated by the Convergence-Confinement and the Hyperstatic  
387 Reaction Methods. *Geotechnical and Geological Engineering*, 37(3): 1435–1452,  
388 <https://doi.org/10.1007/s10706-018-0698-1>.

389 Pöttler R (1990) Green shotcrete in tunnelling: stiffness-strength-deformation. *Shotcrete for Un-*  
390 *derground support*, 4:83-81.

391 Rokahr RB, Lux KH (1987) Einfluss des rheologischen Verhaltens des Spritzbetons auf den  
392 Ausbauwiderstand. *Felsbau* 5:11-18.

393 Schädlich B, Schweiger HF (2014) A new constitutive model for shotcrete. In Hicks MA,  
394 Brinkgreve RBJ, Rohe A, eds. *Numerical Methods in Geotechnical Engineering*. Boca Raton:  
395 CRC Press, 103-108.

396 Schubert P (1988) Beitrag zum rheologischen Verhalten von Spritzbeton. *Felsbau*, 6, 150-153.

397 Spagnoli G, Oreste P, Lo Bianco L. (2016). New equations for estimating radial loads on deep  
398 shaft linings in weak rocks. *International Journal of Geomechanics* 16(6): 06016006, DOI:  
399 [10.1061/\(ASCE\)GM.1943-5622.0000657](https://doi.org/10.1061/(ASCE)GM.1943-5622.0000657).

400 Spagnoli G, Oreste P, Lo Bianco L. (2017) Estimation of shaft radial displacement beyond the  
401 excavation bottom before installation of permanent lining in nondilatant weak rocks with a novel  
402 formulation. *International Journal of Geomechanics*, 17(9): 04017051  
403 [https://doi.org/10.1061/\(ASCE\)GM.1943-5622.0000949](https://doi.org/10.1061/(ASCE)GM.1943-5622.0000949).

- 404 Thomas A (2009) Sprayed Concrete Lined Tunnels. Oxon: Taylor and Francis.
- 405 Yin J (1996) Untersuchungen zum zeitabhängigen Tragverhalten von tiefliegenden Hohlräu-  
406 men im Fels mit Spritzbeton. PhD thesis, Clausthal University of Technology (Germany).
- 407

408 **FIGURE CAPTION**

409 **Fig. 1 Application of shotcrete**

410 **Fig. 2 Voigt-Kelvin creep model ( $\sigma$  is the applied load,  $E$  is the elastic modulus and  $\eta$  is**  
411 **the viscosity coefficient,  $\varepsilon$  is the deformation.**

412 **Fig. 3 Trend of bending moments along the development of the shotcrete lining, in a**  
413 **tunnel cross section, for the D1 case studied in the parametric analysis (A). Detail for**  
414 **the first meter of support length (B). The origin of the lines refers to the centre of the**  
415 **reverse arc and the diagrams consider half of the development of the supporting struc-**  
416 **ture. The diagram shows the trend at the end of the tunnel construction phase ( $t = 0$ ),**  
417 **with the dotted line, and for the 10 stress relief steps considered, until reaching a very**  
418 **high time value (for which  $E_i \approx E_\infty$ ,  $t \approx \infty$ ), shown with the continuous black line.**

419 **Fig. 4 Trend of normal forces along the development of the shotcrete lining, in a tunnel**  
420 **cross section, for the D1 case studied in the parametric analysis (A). Detail for the first**  
421 **meter of support length (B). The origin of the lines refers to the centre of the reverse arc**  
422 **and the diagrams consider half of the development of the supporting structure. The**  
423 **diagram shows the trend at the end of the tunnel construction phase ( $t = 0$ ), with the**  
424 **dotted line, and for the 10 stress relief steps considered, until reaching a very high time**  
425 **value (for which  $E_i \approx E_\infty$ ,  $t \approx \infty$ ), shown with the continuous black line.**

426 **Fig. 5 Trend of safety factors over time at the tunnels type A to H, for the 8 types of**  
427 **sprayed concrete considered.**

428

429 **TABLE CAPTION**

430 **Table 1 Geomechanical parameters of the rock assumed in the calculation for the two**  
431 **values of the RMR indices considered in the parametric analysis.**

432 **Table 2 Types of tunnel considered in the developed parametric analysis.**

433 **Table 3 Types of sprayed concrete considered in the developed parametric analysis.**